ABNUS JOURNAL
Your Research Partner

Jurnal Teknika dan Informatika (JTI)
E-ISSN: 2797-0000 | Vol. 1, No. 2 (2021) | pp. 135–160

Redesign of the Classroom Building Construction at Al-Murqoniyah Vocational School, Hambalang

Era Agita Kabdinoyo[1*], Riesa Syariful Akbar[2]

[1]*Faculty of Engineering and Informatics, Civil Engineering Study Program, Dian Nusantara University, Jakarta, Indonesia*

***Corresponding author:** era.agita.k@undira.ac.id |

Received: 26 September 2021 | Revised: 20 October 2021 | Published: 30 November 2021

Abstract

Purpose: This study aimed to redesign the structure of the Al-Murqoniyah Vocational School building using SNI 1726-2012 for earthquakes and SNI 1726-2012 for concrete. 2847 – 2013.
Research Methodology: A 2-story building structure was planned using the moment-resisting frame system method with structural modeling using a 3-dimensional portal with the help of ETABS version 2013.
Results: Based on the results of the analysis carried out using a structural analysis program, it can be stated that the structural elements of this building are safe in terms of analysis, and the structure of the Al-Murqoniyah Vocational School learning building has been planned according to applicable design principles.
Conclusions: Based on the analysis, the structural elements of the Al-Murqoniyah Vocational School building are safe and compliant with the required design rules. The building has been planned according to SNI 1726-2012 and SNI 2847-2013 standards.
Limitations: The study is limited by the lack of available soil data due to the pandemic, which impacted the foundation analysis. Future studies should include a more detailed substructure analysis and on-site soil investigations.
Contributions: This study provides an in-depth analysis of the structural design for earthquake resistance and concrete structures, which will be useful for future building projects. The findings help improve the design of multi-story school buildings and provide valuable insights into the importance of reinforcement and compliance with SNI standards.

Keywords: *Analysis Reinforcement, Earthquake Resistance, Redesign, Structure Concrete Boned*

How to Cite: Kabdinoyo, E. A., & Akbar, R., S. (2021). Redesign of the Classroom Building Construction at Al-Murqoniyah Vocational School, Hambalang. *Jurnal Teknika dan Informatika (JTI)*, *1*(2), 135–160.
https://doi.org/10.52909/jti.v1i1.15

1. Introduction

Schools play an essential role in the improvement of human life and the overall quality of life, particularly in the context of educational development (Ayuningtyas & Ilman, 2021; Madani, 2019). They provide structured environments where students engage in learning activities, guided by qualified teachers (Hyypiä et al., 2019; Malik & Rizvi, 2018; Wahyuningsih et al., 2021). A key component of these learning environments is the classroom, which significantly influences the quality and effectiveness of education. The classroom not only serves as a space for academic learning but also as a venue for nurturing creativity, critical thinking, and social interaction among students (Amor & Verdugo, 2018;

Syahrial & Sudono, 2021).

Al-Murqoniyah Vocational School, located in Bogor Regency, is a private educational institution that offers vocational training to students. As the school's student population grows each year, there is an increasing need for additional learning spaces to accommodate the rising demand (Ellis & Goodyear, 2016; Park et al., 2016). In response to this challenge, the school plans to build new classrooms. This initiative requires a thorough structural analysis to ensure the new building meets the safety, functionality, and durability standards necessary for educational purposes (Berlian Rms & Wahyuningsih, 2021; Muñoz et al., 2020). The existing Al-Murqoniyah Vocational School structure currently consists of a one-story building that has been in use for several years to support teaching and learning activities. However, with an increase in the number of students, it has become evident that additional classrooms are required to maintain an effective learning environment (Bonem et al., 2020; Sergis et al., 2018; Webster et al., 2015). The construction of a second-floor classroom building is essential for accommodating more students, allowing for better utilization of space, and providing teachers with the flexibility to deliver varied educational materials (Beckers et al., 2015; Cort et al., 2017; Khajehzadeh & Vale, 2016).

The addition of a second floor will not only expand the capacity of the school but also provide a fresh learning atmosphere that is conducive to student engagement and motivation (Saputro & Soleha, 2021; Shernoff et al., 2017). It is expected that the new classrooms will foster an environment that enhances the overall educational experience, in line with the school's curriculum and contemporary learning methods (Kinshuk et al., 2016; Ricardianto et al., 2021; Susanto et al., 2021). The redesign of Al-Murqoniyah Vocational School will feature a two-story building that will house classrooms, a teacher's room, a principal's office, and a laboratory for the electronics engineering program. The construction will follow conventional building methods using reinforced concrete, which is the primary material chosen for its strength, durability, and cost-effectiveness (Hyun et al., 2017; Parmenas, 2021; Younis et al., 2020). This research aims to design the structural components of the new building, ensuring compliance with safety and strength requirements outlined in the relevant national standards (AbouHamad & Abu-Hamd, 2019; Aman et al., 2015; Younis et al., 2018).

The primary goal of this research is to provide a comprehensive structural design for the new two-story building, taking into account the necessary earthquake resistance measures and the requirements for reinforced concrete structures as set forth by Indonesian national standards (Bahmani et al., 2016; van de Lindt et al., 2019). Specifically, the building design will adhere to the guidelines established in SNI 1726:2012, which provides the procedure for earthquake-resistant planning for buildings, and SNI 2847:2013, which outlines the standards for concrete structures in buildings (Setyawati & Aristiyanto, 2021; Setyawati et al., 2021; Susanto & Parmenas, 2021). By following these standards, the design aims to ensure the safety and structural integrity of the new classrooms while also supporting the school's long-term educational goals (Satria, 2021; Solihin, 2021). Through this research, we seek to contribute to the development of safe, efficient, and sustainable educational infrastructures that will enhance the quality of education in the region and provide a positive learning environment for future generations of students at Al-Murqoniyah Vocational School.

2. Literature Review

2.1 Loading Structure

The planning provisions in SNI 2847-2013 procedures are based on the assumption that the structure is designed to support its working load (Kuncoro & Harahap, 2021; Munthe & Nalahuddin, 2019). Article 1, page 7 of the 1983 Indonesian Building Loading Regulations explains the definition of loading as follows:

- Dead load is the weight of all parts of a building that are permanent in nature, including all additional elements, finishes, and permanent equipment that are an integral part of the building.
- Live loads are all loads that occur due to the use of a building, including floor loads that originate from movable loads that cause changes in the floor and roof loading. Specifically, for roofs, live loads include rainwater loads caused by puddles and falling water droplets.
- Wind load is the load acting on a building or part of a building caused by differences in air pressure.
- Earthquake loads are equivalent static loads that act on a building or part of a building and mimic the effects of ground movement caused by an earthquake. The effects of an earthquake on a building's structure are determined using dynamic analysis.

2.2 Stiffness Structure

A rigid frame is a rigid connection used between linear structural arrangements to form vertical and horizontal planes. The vertical plane consists of columns and beams, usually arranged on a square grid (Heriyanto, 2021; Rana & Raheem, 2015).

2.3 Factor Priority And Category Risk Structure

Article 4.1.2 SNI 1726-2012, for various risk categories of building and non-building structures according to Table 2.1, the impact of the planned earthquake on them must be multiplied by the priority factor Ie. Specifically, for building structures with risk category IV, if an entrance door is required for operations and adjacent building structures, the adjacent building structures must be designed according to risk category IV.

Table 1. Risk Category of Buildings and Non-Buildings for Earthquake Loads

Type of Utilization	**Risk Category**
Buildings and non-buildings designated as essential facilities, including but not limited to: • Monumental buildings • School buildings and educational facilities • Hospitals and other health facilities with surgery facilities and emergency units • Fire stations, ambulance facilities, police offices, and emergency vehicle garages	IV

Source: SNI 1726–2012

Based on Table 1, school buildings and educational facilities are classified into Risk Category IV according to SNI 1726–2012. This category indicates that the building has an important function and must remain operational during and after an earthquake (Keke et al., 2021; Mieler & Mitrani-Reiser, 2018). Therefore, the structural planning and design must comply with earthquake-resistant building standards to ensure the safety and reliability of the structure.

2.4 Design Structure Concrete Boned

SNI 2847-2013, concrete is a mixture of Portland cement or other hydraulic cement, fine aggregate, coarse aggregate, and water, with or without additives that form a solid mass. SNI 2847-2013, reinforced concrete is concrete that is reinforced with an area and number of reinforcements that are not less than the minimum value, which is required with or without prestressing, and is planned based on the assumption that both materials work together in resisting the forces applied.

2.5 Analysis And Design

2.5.1 Design

All reinforced concrete structural components must be designed to be sufficiently strong in accordance with the provisions required in the SNI 2847-2013 standard regarding procedures for calculating concrete structures for buildings (Agusinta et al., 2021; Anggraini, 2021), using appropriate load factors and strength reduction factors ϕ.

2.5.2 Modulus Elasticity

The modulus of elasticity of concrete and steel reinforcement is determined as follows:

1. For concrete with a density between 1500 kg/m^3 and 2500 kg/m^3, the modulus of elasticity E_c can be taken as $(w_c)^{1.5} \times 0.0043\sqrt{f'_c}$ (MPa).
2. For normal concrete, E_c can be taken as:

$$E_c = 4700\sqrt{f'_c}$$

3. The modulus of elasticity for non-prestressed reinforcing steel is taken as 200000 MPa.

2.5.3 Provision About Strength And Ability Service

The structure must be planned such that all cross-sections have a minimum design strength equal to the required strength, which is calculated based on a combination of factored loads and forces (Aprillita & Perkasa, 2021; Zhao et al., 2017).

2.6 Required Strength

The required strength of a structural component or cross-section is the strength needed to resist factored loads or moments and internal forces associated with those loads in combination, as specified in SNI 2847-2013 procedures.

The required strength according to Chapter 9.2.1 of SNI 2847-2013 is:

U = 1.4D
U = 1.2D + 1.6L
U = 0.75(1.2D + 1.6L + 1.6W)
U = 0.9D + 1.3W
U = 1.05(D + 0.6L + E)
U = 0.9(D + E)

Where:

- D = dead load,
- L = live load,
- W = wind load,
- E = earthquake load.

2.7 Strong Plan

The design strength of structural components and their cross-sections, with respect to bending, normal load, shear, and torsion behavior (Křístek et al., 2018), shall be taken as the product of the nominal strength, calculated based on the provisions and assumptions from the order method, with a factor reduction strength ϕ. The factor reduction strength ϕ is determined as follows:

- Moment flexible without style axial $\phi = 0.90$
  SNI 2847-2013 chapter 9.3.2.7
- Style axial pull, or moment with style pull $\phi = 0.90$
  SNI 2847-2013 article 9.3.2.1
- Style axial press, or moment with style press $\phi = 0.75$
  SNI 2847-2013 article 9.3.2.2
- Style shift $\phi = 0.75$
  SNI 2847-2013 chapter 9.3.2.3

3. Methodology

Research methodology refers to the stages of research that must be established before problem-solving can be undertaken. This allows for focused research and facilitates the analysis of problems (**Sunarya2018**). The flowchart of the research method is shown in Figure 1.

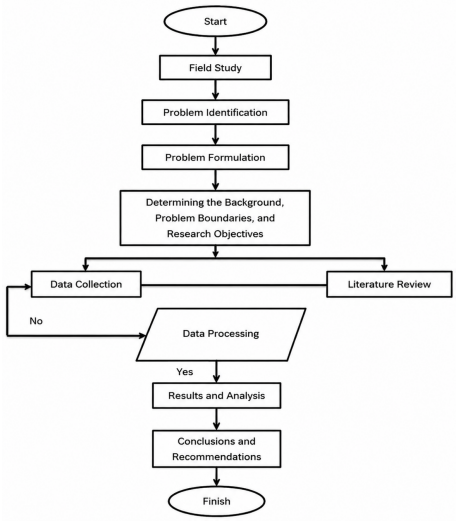

Figure 1. Research Flowchart

Based on Figure 1, the research methodology begins with the "Start" point, followed by a Field Study to identify the problem. The process continues with Problem Identification and Problem Formulation, leading to the step of Determining the Background, Problem Boundaries, and Research Objectives. The next stage involves Data Collection, which then branches into Data Processing or conducting a Literature Review. Afterward, the study proceeds to Results and Analysis, followed by drawing Conclusions and Recommendations, and concludes with the Finish point. This structured approach outlines the flow of the research process, ensuring each step is followed methodically.

3.1 Diagram Flow Design

Structural design must be carried out before the construction process. refers to regulation – regulation, which is related to the structure of multi-storey buildings so that the results are as expected. The flow diagram explains the design of the building structure in detail. In general, the structural design method for the AL-Murqoniyah Vocational School building with a moment frame system is as follows:

1. Collection Data

a. Regulation books, including SNI 1726 – 2012 concerning Procedures for Earthquake Resistance Planning for Building Structures, SNI 2847-2013 on Procedures for Planning Concrete Structures for Buildings, and SNI 03 – 1727 – 1989 on Indonesian Loading Procedures for Houses and Buildings.

b. Based on Figure 2, Building The Al-Murqoniyah Vocational School building is located on Jl. Tajur Tapos RT 21/07 Kp. Tajur Tapos, Hambalang Village, and Sub-district. Citeureup, Kab. Bogor.

Figure 2. Location Building Vocational School Al- Murqoniyah

2. Data Technical Building

Figure 3. Floor plan Building Vocational School Al- Murqoniyah

Based on Figure 3, some information regarding the condition of the floor in the Al-Murqoniyah Vocational School building is as follows:

- Number of Floors : 1 Floor
- Existing Construction Type : Reinforced concrete
- Construction Year : -

- Type Foundation : -
- Size Column : Look Attachment Picture
- Size Beam : Look Attachment Picture
- Quality Concrete : K225
- Reinforcement Quality : Iron reinforcement D = 13 : Steel U40 ($fy = 390$ MPa)
  Reinforcing steel D = 10 : Steel U24 ($fy = 240$ MPa)
- Steel Grade : BJ37
- Soil Condition : -

(a) Standard / Regulation

- American Concrete Institute (ACI 318-99)
- SNI 2847–2013 Tata Method Planning Structure Concrete for Building Building.
- Regulation Loading Indonesia For Building (PPIUG)-1983
- SNI 1726–2012 Tata Method Planning Planning Earthquake For Buildings.
- SNI 1729–2002 Tata Method Planning Structure Steel For Building.

(b) Program / Software

- ETABS Version 18.0.0
- PCACOL
- Spreadsheet Excel

4. Results and Discussion

4.1 Determination Parameter Acceleration Spectral Design

The spectral acceleration response parameters for the highest earthquake are adjusted to class and basic coefficient as follows:

$$S_{ms} = Fa \cdot Ss = 0.9 \cdot 1.0434 = 0.93906 \tag{1}$$

$$S_{M1} = Fv \cdot Sl = 2.4 \cdot 0.4762 = 1.14288 \tag{2}$$

$$S_{DS} = \frac{2}{3} \cdot S_{MS} = \frac{2}{3} \cdot 0.93906 = 0.62604 \tag{3}$$

$$S_{D1} = \frac{2}{3} \cdot 1.14288 = 0.76192 \tag{4}$$

4.2 Equivalent Lateral Static Earthquake Force

The parameters for static earthquake calculation are as follows:

$$T_a = C_t \cdot h^x = 0.0466 \cdot 8.6^{0.9} = 0.32317 \tag{5}$$

$$T = C_u \cdot T_a = 1.4 \cdot 0.32317 = 0.45243 \tag{6}$$

In the ETABS program, the building period for the x and y directions is obtained as $T_x = T_y = 1.12665$

seconds, because $T_a < C_u.T_a$, the building period has met the static limit period criteria.

Table 2. Results of Static Analysis Calculation

Story	HI	Wi	K	Wik	Cv
	M	Kg		kgf-m	
STORY2	8.6	11801.28	1.31	1991717.64	0,75
STORY4	3.8	11238.29	1.31	64884,84	0,25
TOTAL	12.4	23009.57	2.626465	264056,4839	1

4.3 Seismic Base Shear

$$C_s = \frac{S_{DS}}{(\frac{R}{I_e})}$$

$$C_s = 0.62604 = (\frac{8}{1.5}) = 0.117383$$

$$C_s < \frac{S_{D1}}{T(\frac{R}{I_e})} \cdot < \frac{0.76192}{1.126646(\frac{8}{1})} \cdot$$

$$C_s < 0.126801$$

$$C_s > 0.044 \cdot S_{DS} \cdot I_e = 0.044 \cdot 0.117383 \cdot 1.5 = 0.04319$$

Based on the value of C_s above, the value $C_s = 0.051$ is obtained:

$$V_{(x,y)} = C_s \cdot W_t = 0.126801 \cdot 23039.5699 = 2921.443889\text{kg}$$

Table 3. Results Calculation Style Shift Static

Story	Fx	Vx	Fy	Vy
	Kgf	Kgf	Kgf	kgf
STORY 2	2203.58	2203.58	2203,576937	2203,576937
STORY 1	717.87	2921.44	717.8669526	2921.443889

4.4 Analysis And Design Control With Etabs 2013

4.4.1 Nominal Base Shear Force (V)

In the SNI Earthquake 1726 – 2012, it is explained that the final value of the dynamic response of a building structure to the nominated earthquake load due to the influence of the planned earthquake in a certain direction must not be less than 85% of the first variant response value.

Table 4. Mark Base Shear Nominal Static

	V plan	V program	V design
Base Shear	N	N	N
V_x	4206691	4206691	4206691
V_y	4206691	4206691	4206691

Source: Results Calculation, 2014

V plan = Vprogram, so design taken the same with V plan for compared to with V dynamics.

Based on Table 4, the nominal static base shear values in the x and y directions show the same results for the planned value, program value, and design value, namely 4206691 N. This indicates that the structural analysis results obtained from the program are in accordance with the planned and design calculations, so that the structure meets the required base shear criteria.

4.5 Plate Structure Design

4.5.1 Material Data

- Quality Material : Steel, $fy = 390$ MPa
- Concrete, $f'c = 18{,}675$ MPa
- Thick Plate Plan : Floor = 120 mm
- Blanket Concrete : 20 mm
- Reinforcement Plan : diameter 10 mm

4.5.2 Planning Repetition Floor

To determine the need for reinforcement, planning is required with data as follows:

$$\begin{aligned}
\text{Thick plate } (h) &= 120 \text{ mm} \\
\text{Long } (Ln) &= 5000 - 200 = 4800 \text{ mm} \\
\text{Width } (Sn) &= 3000 - 200 = 2800 \text{ mm} \\
\text{Ratio } (\beta) &= \frac{4800}{2800} = 1{,}714 \\
&(\beta \leq 2, \text{ reinforcement 2 Way})
\end{aligned}$$

$$\begin{aligned}
\text{Thick closing } (p) &= 20 \text{ mm} \\
\text{D. reinforcement } (\phi p) &= 10 \text{ mm}
\end{aligned}$$

$$\begin{aligned}
\text{Tall effective, } d_x &= h - p - \frac{1}{2} \cdot \phi px \\
&= 120 - 20 - \frac{1}{2} \cdot 10 \\
&= 95 \text{ mm}
\end{aligned}$$

$$\begin{aligned}
d_y &= h - p - \phi px - \frac{1}{2} \cdot \phi py \\
&= 120 - 20 - 10 - 5 \\
&= 85 \text{ mm}
\end{aligned}$$

$$\begin{aligned}
\text{Strong press } (fc') &= 18{,}675 \text{ MPa} \\
\text{Yield strength } (fy) &= 390 \text{ MPa}
\end{aligned}$$

From the data above, we obtain:

$$\rho_b = \frac{0.85\beta_1 f_c'}{f_y + f_c} = \frac{0.85 \times 1.30 \times 600}{600 + 390} = 0.020976657 \tag{7}$$

$$\rho_{\max} = 0.75 \times \rho_b = 0.75 \times 0.020976657 = 0.015725743 \tag{8}$$

Based on SNI 2847:2013 Article 7.12.2.1, the volume of reinforcement and the temperature provides at least the following reinforcement ratio to gross concrete area:

- For slabs with reinforcement of 280 MPa or 350 MPa, the ratio is 0.002
- For slabs with reinforcement of 420 MPa, the ratio is 0.0018. For slabs with reinforcement of 240 MPa, the ratio is 0.002.
- If the reinforcement exceeds 420 MPa, measured at the yield strength strain of 0.35%, the ratio is $0.0018 \times 420/f_y$

4.6 Example of Reinforced Concrete Beam Design in Direction X (per 1 meter)

b = 1000 mm
dx = 95 mm Mu = 8180000 Nmm
$Mn = \frac{Mu}{\phi}$

$$\begin{aligned} R_n &= \frac{M_n}{b \cdot d_x^2} \\ &= \frac{9088888.89}{1000 \cdot 95^2} \\ &= 1.007079101 \text{ N/mm}^2 \end{aligned}$$

$$\begin{aligned} m_d &= \frac{fy}{0.85 \cdot fc'} \\ &= \frac{390}{0.85 \cdot 18.675} \\ &= 24.56886369 \text{ MPa} \end{aligned}$$

$$\begin{aligned} \rho &= \frac{1}{m}\left[1 - \sqrt{1 - \frac{2.m.R_n}{fy}}\right] \\ &= 0.002669817 \end{aligned}$$

Based on SNI 03-2842-2013

$$\rho < \rho_{max}$$
$$0.002669817 < 0.015725743 \text{ (Single reinforcement is required)}$$

$$\rho > \rho_{min}$$
$$0.002669817 > 0.0018 \text{ (Used } \rho = 0.015725743)$$

$$\begin{aligned} As_{required} &= \rho \cdot b \cdot d_x \\ &= 0.015725743 \cdot 1000 \text{ mm} \cdot 95 \text{ mm} \\ &= 253.6325731 \text{ mm}^2 \end{aligned}$$

$$\begin{aligned} \text{Area of reinforcement} &= 0.25\pi D^2 \\ &= 0.25 \times 3.14 \times 10^2 \\ &= 78.5 \text{ mm}^2 \end{aligned}$$

$$\begin{aligned} n &= \frac{As_{required}}{\text{Area of reinforcement}} \\ &= \frac{253.6326}{78.5} \\ &= 3.23 \text{ bars} \end{aligned}$$

Therefore, 4 reinforcement bars are used.

$$\begin{aligned} S &\leq \frac{0.25\pi D^2 \cdot b}{As_{required}} \\ &\leq \frac{0.25 \times 3.14 \times 10^2 \times 1000}{253.6326} \\ &\leq 309.502 \text{ mm} \end{aligned}$$

Based on SNI 2847:2013 Clause 13.3.2, the reinforcement spacing at the critical section shall not exceed twice the slab thickness; therefore, a spacing of 150 mm is used.

$$\begin{aligned} As_{provided} &= \text{area of } \phi \text{ reinforcement} \cdot \text{number of bars} \\ &= \left(\frac{1}{4}\pi \cdot 10^2\right) \cdot 7 \\ &= 549.5 \text{ mm}^2 \end{aligned}$$

Requirement of Reinforcement Ratio :

$$\begin{aligned}\rho &= \frac{As}{b \times d} \\ &= \frac{549.5}{1000 \times 95} \\ &= 0.00578\end{aligned}$$

$$(\rho_{min} < \rho < \rho_{max}) \qquad \text{...OK}$$

$$\begin{aligned}&S_{installed} \leq 2t \\ &150 \text{ mm} < 240 \text{ mm} \qquad \text{...OK}\end{aligned}$$

Check the nominal strength of the section:

$$\begin{aligned}a &= \frac{As \cdot fy}{0.85 \cdot fc' \cdot b} \\ &= \frac{549.5 \times 390}{0.85 \times 18.675 \times 1000} \\ &= 13.5 \text{ mm}\end{aligned}$$

Determine the location of the neutral axis:

$$\begin{aligned}c &= \frac{a}{\beta_1} \\ &= \frac{13.5}{0.85} \\ &= 15.88 \text{ mm}\end{aligned}$$

Reinforcement strain control:

$$\begin{aligned}\varepsilon_s &= \frac{d-c}{c} \cdot 0.003 \\ &= \frac{95-15.88}{15.88} \cdot 0.003 \\ &= 0.0149\end{aligned}$$

$$\begin{aligned}\varepsilon_y &= \frac{fy}{Es} \\ &= \frac{390}{200000} \\ &= 0.00195\end{aligned}$$

The above calculation results in $\varepsilon_s \geq \varepsilon_y$, therefore the reinforcing steel has yielded according to the assumption $f_s = fy = 390$ MPa. Thus, the moment capacity can be determined.

$$\begin{aligned}Mn &= As \cdot fy\left(d - \frac{a}{2}\right) \\ &= 594.5 \times 390\left(95 - \frac{13.5}{2}\right) \\ &= 20461203.75 \text{ Nmm}\end{aligned}$$

$$\begin{aligned}Mu &= \phi \cdot Mn \\ &= 0.9 \times 20461203.75 \\ &= 18415083.38 \text{ Nmm}\end{aligned}$$

$$Mu_{required} \leq Mu_{capacity}$$

$$8180000 \text{ Nmm} \leq 18415083.38 \text{ Nmm}$$

Therefore, D10–150 reinforcement is used for reinforcement in the X direction (support), and this section can be used.

4.7 Calculation Results

Based on the results of the planned reinforcement calculations used for the parking slab, the reinforcement used is obtained. The results of the slab reinforcement analysis can be seen in the table.

Table 5. Results of Flexural Reinforcement Analysis of Parking Floor Slab P2

Reinforcement	Direction	Moment (Nmm)	As (mm^2)	Installed Reinforcement
Field	X	5701000	549.5	D10–150
	Y	3899000	549.5	D10–150
Support	X	4042000	549.5	D10–150
	Y	3290500	549.5	D10–150

Based on Table 5, the flexural reinforcement analysis results for the parking floor slab P2 show the required reinforcement area and the corresponding reinforcement detailing in both the X and Y directions for field and support regions. In the field area, the bending moments reach 5,701,000 Nmm in the

X-direction and 3,899,000 Nmm in the Y-direction, both requiring a reinforcement area (As) of 549.5 mm^2. Similarly, in the support region, the moments are 4,042,000 Nmm (X-direction) and 3,290,500 Nmm (Y-direction), which also result in the same required steel area of 549.5 mm^2. Based on these requirements, a uniform reinforcement arrangement of D10–150 is used for all cases. This indicates that the selected reinforcement configuration is sufficient to resist the bending moments in both directions and both structural zones, ensuring structural adequacy and constructability consistency across the slab.

4.8 Calculation Results

Based on the results of the analysis and calculations, the number of flexural reinforcements for the beam is obtained as follows:

Table 6. Number of Beam Flexural Reinforcements

Beam	Support		Field	
	Top	Bottom	Top	Bottom
B200X400	3D13	3D13	3D13	3D13

Based on Table 6, the flexural reinforcement design for beam B200×400 shows a uniform reinforcement arrangement for both support and field regions. The beam requires 3D13 reinforcement at both the top and bottom layers, with no variation between the support and field zones. This indicates that the bending demand along the beam is relatively consistent, allowing the same reinforcement configuration to be used throughout the span. The provided reinforcement layout ensures adequate flexural capacity in both positive and negative moment regions, while also simplifying construction and detailing (Al-Osta et al., 2017; Rabi et al., 2019).

4.9 Planning of beam Shear Reinforcmenet Using Capacity Moment Method

Based on SNI 2847-2013 Clause 21.6.2.2, the design shear due to earthquake in the beam is calculated by assuming plastic hinges are formed at the beam ends and the flexural reinforcement stress reaches 1.25fy and the beam end reduction reinforcement is equal to 1.

1. Beam end moment capacity when the structure sways to the right (Left Support).

$$As = 398.00 \text{ mm}^2$$

$$\begin{aligned} a_{pr} &= \frac{1.25.As.fy}{0.85.fc'.b} \\ &= \frac{1.25 \times 398 \times 390}{0.85 \times 18.675 \times 200} \\ &= 61.11 \end{aligned}$$

$$\begin{aligned} Mpri^* &= 1.25.As.fy\left(d - \frac{a_{pr}}{2}\right) \\ &= 1.25 \times 398.13 \times 390\ (363.5 - 61.11/2) \\ &= 64598426.80 \text{ Nmm} \end{aligned}$$

$$As = 398.00 \text{ mm}^2$$

$$
\begin{aligned}
a_{pr} &= \frac{1.25.As.fy}{0.85.fc'.b} \\
&= \frac{1.25 \times 398 \times 390}{0.85 \times 18.675 \times 200} \\
&= 61.11
\end{aligned}
$$

$$
\begin{aligned}
Mpri^{*} &= 1.25.As.fy\left(d - \frac{a_{pr}}{2}\right) \\
&= 1.25 \times 398.13 \times 390\ (363.5 - 61.11/2) \\
&= 64598426.80\ \text{Nmm}
\end{aligned}
$$

2. Beam end moment capacity when the structure sways to the left (Right Support).

$$As = 398.00\ \text{mm}^2$$

$$
\begin{aligned}
a_{pr} &= \frac{1.25.As.fy}{0.85.fc'.b} \\
&= \frac{1.25 \times 398 \times 390}{0.85 \times 18.675 \times 200} \\
&= 61.11
\end{aligned}
$$

$$
\begin{aligned}
Mpri^{*} &= 1.25.As.fy\left(d - \frac{a_{pr}}{2}\right) \\
&= 1.25 \times 398.13 \times 390\ (363.5 - 61.11/2) \\
&= 64598426.80\ \text{Nmm}
\end{aligned}
$$

$$As = 398.00\ \text{mm}^2$$

$$
\begin{aligned}
a_{pr} &= \frac{1.25.As.fy}{0.85.fc'.b} \\
&= \frac{1.25 \times 398 \times 390}{0.85 \times 18.675 \times 200} \\
&= 61.11
\end{aligned}
$$

$$
\begin{aligned}
Mpri^{*} &= 1.25.As.fy\left(d - \frac{a_{pr}}{2}\right) \\
&= 1.25 \times 398.13 \times 390\ (363.5 - 61.11/2) \\
&= 64598426.80\ \text{Nmm}
\end{aligned}
$$

3. Shear force diagram. Shear reactions at the right and left ends of the beam due to gravity forces acting on the structure. The results of the structural analysis using the ETABS 2013 program.

   Load combination:

$$Wu = 1.2\ DL + 1.0\ LL$$

   Obtained:

$$V_{g,ki} = \frac{W_u\ L_n}{2} = 9291.00\ \text{N}$$

$$V_{g,ka} = \frac{W_u\ L_n}{2} = 9291.00\ \text{N}$$

4. Structure sways to the right.

$$\begin{aligned} Ve &= \frac{M_{pr}^{+} + M_{pr}^{-}}{L_n} \\ &= 30045.78\ \text{N} \end{aligned}$$

$$\begin{aligned} \text{Total shear reaction at the left beam end} &= 30045.78 + 9291.00 \\ &= 39336.78\ \text{N} \end{aligned}$$

$$\begin{aligned} \text{Total shear reaction at the right beam end} &= 30045.78 - 9291.00 \\ &= 20754.78\ \text{N} \end{aligned}$$

   Structure sways to the left.

$$\begin{aligned} Ve &= \frac{M_{pr}^{+} + M_{pr}^{-}}{L_n} \\ &= 30045.78\ \text{N} \end{aligned}$$

$$\begin{aligned} \text{Total shear reaction at the left beam end} &= 30045.78 + 9291.00 \\ &= 39336.78\ \text{N} \end{aligned}$$

$$\begin{aligned}\text{Total shear reaction at the right beam end} &= 30045.78 - 9291.00 \\ &= 20754.78 \text{ N}\end{aligned}$$

5. Stirrups for shear force. SNI 03-2847-2012 Clause 23.3.4(2): $Vc = 0$ in shear design at the plastic hinge region.

   The shear force *Ve* due to plastic hinges at the beam ends exceeds $\frac{1}{2}$ (or more) of the maximum required shear strength, therefore the shear reinforcement must be designed by:

$$Vu_{max} = 12425.62 \text{ N}$$

$$\begin{aligned}Vs = \frac{V_u}{\phi} - V_c = V_s &= \frac{12425.62}{0.75} - 0 \\ &= 16567.49 \text{ N}\end{aligned}$$

   Maximum V_s:

$$\begin{aligned}V_{s,max} &= \frac{2\sqrt{fc'}}{3} b_w d \\ &= \frac{2\sqrt{30}}{3} \times 200 \times 363.5 \\ &= 209446.66 \text{ N}\end{aligned}$$

   The stirrup diameter used is D10 with 2 legs ($Av = 157$ mm^2)

$$\begin{aligned}Av &= 0.25 \times 3.14 \times 10^2 \times 2 \\ &= 157 \text{ mm}^2\end{aligned}$$

$$\begin{aligned}s &= \frac{Av.fy.d}{Vs} \\ &= \frac{157.390.363.5}{209446.66} \\ &= 106.266 \text{ mm}\end{aligned}$$

The D10 reinforcement steel with reinforcement spacing of 100 mm is used.

$$
\begin{aligned}
Vs &= \frac{Av.fy.d}{s} \\
&= \frac{157.390.363.5}{100} \\
&= 222571.05 \text{ N}
\end{aligned}
$$

SNI 2847-2013 Clause 21.5.3(2): The maximum spacing along the beam shall not exceed:

$$\frac{d}{4}$$

6.D longitudinal bar diameter

150 mm

Thus, D10 stirrups with 2 legs are used with a spacing of 100 mm in the region along 2h (=800 mm).

Stirrups in the region outside the plastic hinge

$$
\begin{aligned}
Vc &= \frac{\sqrt{fc'}}{6} b_w d \\
&= \frac{\sqrt{18.675}}{6} \times 200 \times 363.5 \\
&= 52361.67 \text{ N}
\end{aligned}
$$

$$
\begin{aligned}
Vs &= \frac{V_u}{\phi} - V_c \\
&= \frac{39336.78}{0.75} - 52361.67 \\
&= 87.37 \text{ N}
\end{aligned}
$$

The stirrup reinforcement diameter used is D10 with 2 legs ($Av = 157$ mm^2)

$$
\begin{aligned}
Av &= 0.25 \times 3.14 \times 10^2 \times 2 \\
&= 157 \text{ mm}^2
\end{aligned}
$$

$$
\begin{aligned}
s &= \frac{Av.fy.d}{Vs} \\
&= \frac{157.390.363.5}{87.37} \\
&= 493.79 \text{ mm}
\end{aligned}
$$

The D10 reinforcement steel with reinforcement spacing of 150 mm is used.

4.10 Column Structure Design

Column Flexural Reinforcement Design

Interaction Diagram Method

The flexural reinforcement design using the interaction diagram method utilizes the pcaCOL program to create the interaction diagram.

Table 7. Interaction Diagram Values of Column 200x250 from ETABS

Story	Column	Load	P	V2	V3	M2	M3
STORY2	C26	COMB4	279.04	-17.09	4.41	8.359	-32.259
STORY2	C26	COMB3	283.10	-17.08	-4.45	-8.457	-32.227
STORY1	C26	COMB2	527.06	-5.03	-0.06	0.016	-1.624
STORY1	C26	COMB2	526.63	-5.03	-0.06	0.035	-0.115

Based on Table 7, the interaction diagram values of column 200x250 obtained from the ETABS analysis show that the largest axial load occurs in STORY1 for column C26 under load combination COMB2 with a value of 527.06, while the largest moment in the M3 direction occurs in STORY2 for column C26 under load combination COMB4 with a value of -32.259. These results indicate that the column is subjected to varying axial and moment forces depending on the applied load combinations (Abdullah, 2021; Dang et al., 2018).

Table 8. Interaction Diagram Values of Column 150x150 from ETABS

Story	Column	Load	P	V2	V3	M2	M3
STORY2	C43	COMB12	20.540	-3.22	1.05	1.997	-6.095
STORY2	C43	COMB4	37.650	-3.22	1.11	2.108	-6.091
STORY1	C35	COMB8	145.58	1.08	-3.51	-2.314	0.622
STORY1	C35	COMB8	145.33	1.08	-3.51	-1.086	0.242

Based on Table 8, the interaction diagram values of column 150x150 from the ETABS analysis indicate that the largest axial load occurs in STORY1 for column C35 under load combination COMB8 with a value of 145.58. Meanwhile, the largest moment in the M3 direction occurs in STORY2 for column C43 under load combination COMB12 with a value of -6.095. The results show that the internal forces acting on the columns vary according to the structural loading conditions and load combinations applied.

From the results of the program analysis, the axial force (P) and moment acting on the column can be identified and the interaction diagram can be illustrated as follows:

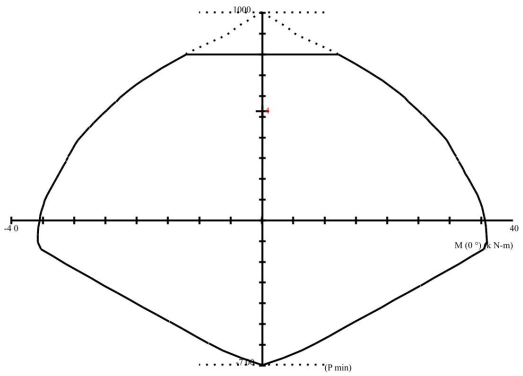

Figure 4. Diagram Interaction Column 200x250

Figure 4 shows the relationship between torque (M) and power (P) in a mechanical system. The X-axis represents torque in N·m, and the Y-axis represents power in kW. The dotted lines indicate critical points, including the minimum power output (P min) where performance starts to decline. The red arrow marks a significant transition point in the graph, highlighting key torque values that affect power efficiency.

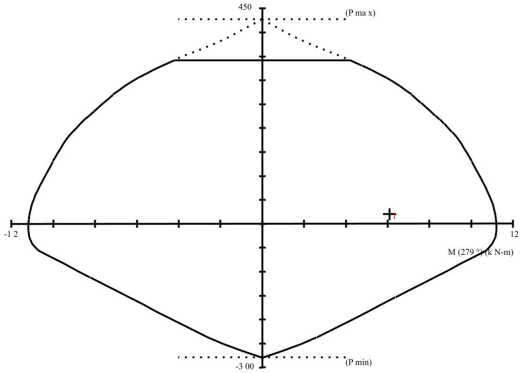

Figure 5. Diagram Interaction Column 150x150

Based on Figure 5, the graph illustrates the relationship between torque (M) and power (P) in a mechanical system. The X-axis represents torque in N·m, and the Y-axis represents power in kW. The dotted lines indicate the maximum power (P max) and minimum power (P min) points, with the critical transition points marking where the power output changes significantly. The red arrow highlights the significant point where the torque and power values intersect, providing important insight into the performance of the system.

Based on the results obtained, the interaction produces the amount of reinforcement according to the image below:

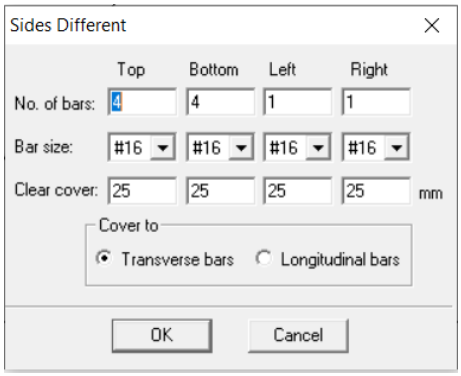

Figure 6. Column 200x250 Installed reinforcement 10D16

Based on Figure 6, the image shows a settings window for defining reinforcement parameters in a structural analysis or design program. The "Sides Different" menu allows the user to customize the number of bars for each side of the structure (Top, Bottom, Left, and Right). It also specifies the size of the bars (e.g., #16) and the clear cover thickness, all given in millimeters (mm). The user can select whether the clear cover applies to transverse bars or longitudinal bars. These settings are crucial for accurate modeling of reinforcement placement in structural elements.

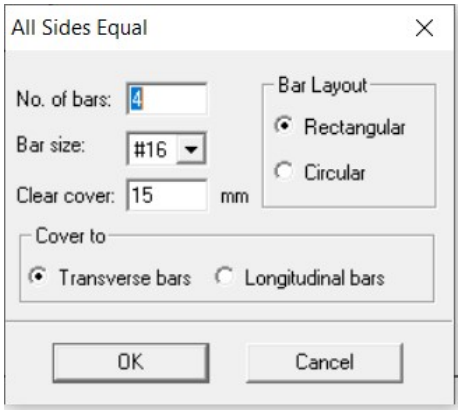

Figure 7. Column 150x150 Installed reinforcement 4D16

Based on Figure 7, the image shows a settings window for defining reinforcement parameters in a structural analysis or design program, with the option for "All Sides Equal." This menu allows the user to set the same number of bars (e.g., 4) and size (e.g., #16) for all sides of the structural element. The user can choose the bar layout as either rectangular or circular. Additionally, the clear cover thickness is set at 15 mm, and the user can select whether the clear cover applies to transverse bars or longitudinal bars. These settings ensure uniform reinforcement configuration for the element.

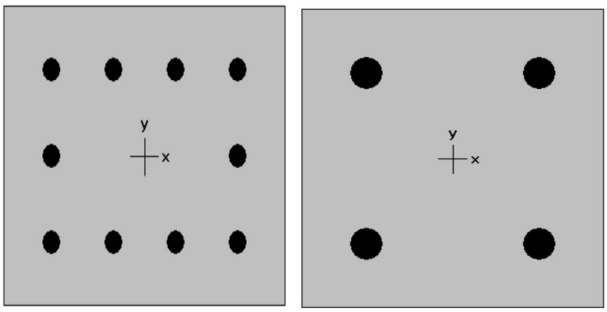

a) b)

Figure 8. a. (4D16150X150) b. (10D16 K200X250)

5. Conclusions

Based on the results of the analysis and calculations that have been carried out in the redesign of the construction of the Al-Murqoniyah Vocational School classroom, Hambalang, it can be concluded that the number of reinforcements obtained from the analysis results for plate reinforcement (t=120 mm) using D10-100 reinforcement for each support and field, in the beam structure ($200 \times 400mm$) using 3D13 flexural reinforcement in the compression area and 3D13 in the tension area, with the stirrup distance at the support being D10-100 in the support area and D10-150 in the field area, as well as for the flexural reinforcement of the column ($200 \times 250mm$) 10D16 reinforcement and D10-100 stirrup reinforcement are used in the support area and D10-150 reinforcement in the field area. Based on the results of the analysis carried out using a structural analysis program, it can be stated that the structural elements of this building are safe in terms of analysis, and the structure of the Al-Murqoniyah Vocational School learning building has been planned according to the applicable design rules, namely those regulated in SNI 1726 - 2012 concerning Procedures for Planning Earthquake Resistance for Buildings and SNI 2847 – 2013 concerning Procedures for Planning Concrete Structures for Buildings.

Acknowledgements

The authors would like to express their gratitude to the Faculty of Engineering and Informatics at Dian Nusantara University for providing the resources and support throughout the study. We also thank the construction team and all those involved in the planning process at Al-Murqoniyah Vocational School.

Author Contributions

EAK conceptualized and designed the study, performed the data collection, analyzed the results, contributed to the writing of the original draft. RSA contributed to the analysis and interpretation of the data, and reviewed the manuscript. Both authors approved the final manuscript and agreed on the contents for publication.

Conflicts of Interest

The authors declare that there is no conflict of interest regarding the publication of this study. This research was conducted independently, and no financial or personal relationships influenced the results or interpretation of the findings.

References

Abdullah, M. A. F. (2021). Analysis of consumer motives in purchasing decisions and the use of instant cooking seasonings. *Jurnal Bisnis, Ekonomi, Manajemen, Dan Kewirausahaan*, *1*(1), 27–35. https://doi.org/10.52909/jbemk.v1i1.24

AbouHamad, M., & Abu-Hamd, M. (2019). Framework for construction system selection based on life cycle cost and sustainability assessment. *Journal of Cleaner Production*, *241*, 118397. https://doi.org/10.1016/j.jclepro.2019.118397

Agusinta, L., Nugroho, A. E., Fachrial, P., & Suryawan, R. F. (2021). Assessment model of employee competence, ground support equipment effectiveness, and satisfaction on service quality. *Jurnal Transportasi, Logistik, dan Aviasi*, *1*(1), 55–69. https://doi.org/10.52909/jtla.v1i1.37

Al-Osta, M. A., Isa, M. N., Baluch, M. H., & Rahman, M. K. (2017). Flexural behavior of reinforced concrete beams strengthened with ultra-high performance fiber reinforced concrete. *Construction and Building Materials*, *134*, 279–296. https://doi.org/10.1016/j.conbuildmat.2016.12.094

Aman, M., Nadeem, H., & Khaled, E. S. (2015). Seismic performance and cost-effectiveness of high-rise buildings with increasing concrete strength. *The Structural Design of Tall and Special Buildings*, *24*(4), 257–279. https://doi.org/10.1002/tal.1165

Amor, A. M., & Verdugo, M. A. (2018). Quality of life and its role for guiding practices in the social and educational services from a systems perspective. *Człowiek-Niepełnosprawność-Społeczeństwo*, *41*, 15–27. https://doi.org/10.5604/01.3001.0012.7817

Anggraini, D. (2021). The impact of covid-19 on stock price changes. *Jurnal Bisnis, Ekonomi, Manajemen, Dan Kewirausahaan*, *1*(1), 1–18. https://doi.org/10.52909/jbemk.v1i1.22

Aprillita, D., & Perkasa, D. H. (2021). The impact of the covid-19 pandemic on consumer purchasing power in the online retail sectors. *Jurnal Bisnis, Ekonomi, Manajemen, Dan Kewirausahaan*, *1*(1), 19–26. https://doi.org/10.52909/jbemk.v1i1.23

Ayuningtyas, B., & Ilman, S. (2021). Ip camera surveillance system using an android application based on arduino. *Jurnal Teknika Dan Informatika*, *1*(1), 1–18. https://doi.org/10.52909/jti.v1i1.6

Bahmani, P., van de Lindt, J. W., Gershfeld, M., Mochizuki, G. L., Pryor, S. E., & Rammer, D. (2016). Experimental seismic behavior of a full-scale four-story soft-story wood-frame building with retrofits. i: Building design, retrofit methodology, and numerical validation. *Journal of Structural Engineering*, *142*(4), E4014003.

Beckers, R., der Voordt, T. V., & Dewulf, G. (2015). A conceptual framework to identify spatial implications of new ways of learning in higher education. *Facilities*, *33*(1–2), 2–19. https://doi.org/10.1108/F-02-2013-0013

Berlian Rms, A., & Wahyuningsih, E. (2021). Analysis of frictional energy generation between train wheels and rails. *Jurnal Teknika Dan Informatika*, *1*(1), 46–61. https://doi.org/10.52909/jti.v1i1.10

Bonem, E. M., Fedesco, H. N., & Zissimopoulos, A. N. (2020). What you do is less important than how you do it: The effects of learning environment on student outcomes. *Learning Environments Research*, *23*(1), 27–44. https://doi.org/10.1007/s10984-019-09289-8

Cort, C., Cort, G., & Williams, R. (2017). The challenge of making buildings flexible: How to create campuses that adapt to changing needs. *Planning for Higher Education*, *45*(4), 96–104.

Dang, H. V., Lee, K., Han, S. W., & Kim, S. J. (2018). Experimental assessment of the effects of biaxial bending moment and axial force on reinforced concrete corner columns. *Structural Concrete*, *19*(4), 1063–1078. https://doi.org/10.1002/suco.201700211

Ellis, R. A., & Goodyear, P. (2016). Models of learning space: Integrating research on space, place and learning in higher education. *Review of Education*, *4*(2), 149–191. https://doi.org/10.1002/rev3.3056

Heriyanto, D. (2021). The impact of service quality and compensation on crew satisfaction in manning companies. *Jurnal Transportasi, Logistik, dan Aviasi*, *1*(1), 31–41. https://doi.org/10.52909/jtla.v1i1.35

Hyun, J., Ediger, R., & Lee, D. (2017). Students' satisfaction on their learning process in active learning and traditional classrooms. *International Journal of Teaching and Learning in Higher Education*, *29*(1), 108–118.

Hyypiä, M., Sointu, E., Hirsto, L., & Valtonen, T. (2019). Key components of learning environments in creating a positive flipped classroom course experience. *International Journal of Learning, Teaching and Educational Research*, *18*(13), 61–86. https://doi.org/10.26803/ijlter.18.13.4

Keke, Y., Tobing, N. G. L., & Tanjung, I. (2021). The effect of occupational safety and health on employee performance at pt. angkasa kargo. *Jurnal Transportasi, Logistik, dan Aviasi*, *1*(1), 42–54. https://doi.org/10.52909/jtla.v1i1.36

Khajehzadeh, I., & Vale, B. (2016). Shared student residential space: A post occupancy evaluation. *Journal of Facilities Management*, *14*(2), 102–124. https://doi.org/10.1108/JFM-09-2014-0031

Kinshuk, Chen, N. S., Cheng, I. L., & Chew, S. W. (2016). Evolution is not enough: Revolutionizing current learning environments to smart learning environments. *International Journal of Artificial Intelligence in Education*, *26*(2), 561–581. https://doi.org/10.1007/s40593-016-0108-x

Křístek, V., Průša, J., & Vítek, J. L. (2018). Torsion of reinforced concrete structural members. *Solid State Phenomena*, *272*, 178–184. https://doi.org/10.4028/www.scientific.net/SSP.272.178

Kuncoro, H., & Harahap, V. (2021). Effect of electronic flight bag usage and safety culture on flight safety performance at pt. garuda indonesia. *Jurnal Transportasi, Logistik, dan Aviasi*, *1*(1), 18–30. https://doi.org/10.52909/jtla.v1i1.34

Madani, R. A. (2019). Analysis of educational quality, a goal of education for all policy. *Higher Education Studies*, *9*(1), 100–109.

Malik, R. H., & Rizvi, A. A. (2018). Effect of classroom learning environment on students' academic achievement in mathematics at secondary level. *Bulletin of Education and Research*, *40*(2), 207–218.

Mieler, M. W., & Mitrani-Reiser, J. (2018). Review of the state of the art in assessing earthquake-induced loss of functionality in buildings. *Journal of Structural Engineering*, *144*(3), 04017218.

Muñoz, V. A., Carby, B., Abella, E. C., Cardona, O. D., López-Marrero, T., Marchezini, V., et al. (2020). Success, innovation and challenge: School safety and disaster education in south america and the caribbean. *International Journal of Disaster Risk Reduction*, *44*, 101395. https://doi.org/10.1016/j.ijdrr.2019.101395

Munthe, A. T., & Nalahuddin, M. (2019). Coupling beam design with special moment frame and special reinforced concrete shear walls. *Neutron*, *18*(2), 28–41. https://doi.org/10.29138/neutron.v18i2.75

Park, H., Buchmann, C., Choi, J., & Merry, J. J. (2016). Learning beyond the school walls: Trends and implications. *Annual Review of Sociology*, *42*(1), 231–252. https://doi.org/10.1146/annurev-soc-081715-074341

Parmenas, N. H. (2021). Strategies for maintaining employee well-being during the covid-19 pandemic. *Journal of Economics, Management, Entrepreneurship, & Business*, *1*(1), 15–31. https://doi.org/10.52909/jemeb.v1i1.3

Rabi, M., Cashell, K. A., & Shamass, R. J. E. S. (2019). Flexural analysis and design of stainless steel reinforced concrete beams. *Engineering Structures*, *198*, 109432. https://doi.org/10.1016/j.engstruct.2019.109432

Rana, D., & Raheem, J. (2015). Seismic analysis of regular and vertical geometric irregular rcc framed building. *International Research Journal of Engineering and Technology*, *2*(04), 2395–0056.

Ricardianto, P., Sakti, R. F. J., Sembiring, H. F. A., & Abidin, Z. (2021). Safety performance analysis of state and commercial ships in accordance with solas 1974. *Journal of Economics, Management, Entrepreneurship, & Business*, *1*(1), 1–14. https://doi.org/10.52909/jemeb.v1i1.2

Saputro, A., & Soleha, I. (2021). Analysis of the performance of extraction-condensing turbine unit 1 at bablean power plant. *Jurnal Teknika Dan Informatika*, *1*(1), 62–79. https://doi.org/10.52909/jti.v1i1.11

Satria, B. (2021). The effect of transformational leadership and work motivation on employee performance at pt. xyz. *Jurnal Bisnis, Ekonomi, Manajemen, Dan Kewirausahaan*, *1*(1), 36–47. https://doi.org/10.52909/jbemk.v1i1.25

Sergis, S., Sampson, D. G., & Pelliccione, L. (2018). Investigating the impact of flipped classroom on students' learning experiences: A self-determination theory approach. *Computers in Human Behavior*, *78*, 368–378. https://doi.org/10.1016/j.chb.2017.08.011

Setyawati, A., & Aristiyanto, F. K. (2021). Improving discipline through apron movement control (amc) at pt angkasa pura i adi soemarmo airport. *Jurnal Transportasi, Logistik, dan Aviasi*, *1*(1), 1–17. https://doi.org/10.52909/jtla.v1i1.33

Setyawati, A., Huda, M. N., Suripno, S., & Tannady, H. (2021). Analysis of integrated bus terminal services and their impact on customer satisfaction at pulo gebang. *Journal of Economics, Management, Entrepreneurship, & Business*, *1*(1), 44–55. https://doi.org/10.52909/jemeb.v1i1.5

Shernoff, D. J., Ruzek, E. A., & Sinha, S. (2017). The influence of the high school classroom environment on learning as mediated by student engagement. *School Psychology International*, *38*(2), 201–218. https://doi.org/10.1177/0143034316666413

Solihin, A. (2021). The effect of workload, compensation, and career development on employee loyalty at pt. abc. *Jurnal Bisnis, Ekonomi, Manajemen, Dan Kewirausahaan*, *1*(1), 48–58. https://doi.org/10.52909/jbemk.v1i1.26

Susanto, P. C., & Parmenas, N. H. (2021). Development of a succession planning model for insurance subsidiaries. *Journal of Economics, Management, Entrepreneurship, & Business*, *1*(1), 56–75. https://doi.org/10.52909/jemeb.v1i1.16

Susanto, P. C., Suryawan, R. F., Hartono, H., & Purwoko, B. A. (2021). Analysis of accident-prone areas along the ciawi–puncak road, bogor. *Journal of Economics, Management, Entrepreneurship, & Business*, *1*(1), 32–43. https://doi.org/10.52909/jemeb.v1i1.4

Syahrial, E., & Sudono, R. H. (2021). Cooling load analysis of a new building at pmi bogor hospital using the cltd method. *Jurnal Teknika Dan Informatika*, *1*(1), 34–45. https://doi.org/10.52909/jti.v1i1.9

van de Lindt, J. W., Furley, J., Amini, M. O., Pei, S., Tamagnone, G., Barbosa, A. R., et al. (2019). Experimental seismic behavior of a two-story clt platform building. *Engineering Structures*, *183*, 408–422. https://doi.org/10.1016/j.engstruct.2018.12.079

Wahyuningsih, E., Widodo, S., & Rahmanto, R. (2021). Prototype manufacture of the arjuno autobost covid-19 robot. *Jurnal Teknika Dan Informatika*, *1*(1), 19–33. https://doi.org/10.52909/jti.v1i1.8

Webster, C. A., Russ, L., Vazou, S., Goh, T. L., & Erwin, H. (2015). Integrating movement in academic classrooms: Understanding, applying and advancing the knowledge base. *Obesity Reviews*, *16*(8), 691–701. https://doi.org/10.1111/obr.12285

Younis, A., Ebead, U., & Judd, S. (2018). Life cycle cost analysis of structural concrete using seawater, recycled concrete aggregate, and gfrp reinforcement. *Construction and Building Materials*, *175*, 152–160. https://doi.org/10.1016/j.conbuildmat.2018.04.183

Younis, A., Ebead, U., Suraneni, P., & Nanni, A. (2020). Cost effectiveness of reinforcement alternatives for a concrete water chlorination tank. *Journal of Building Engineering*, *27*, 100992. https://doi.org/10.1016/j.jobe.2019.100992

Zhao, O., Afshan, S., & Gardner, L. (2017). Structural response and continuous strength method design of slender stainless steel cross-sections. *Engineering Structures*, *140*, 14–25. https://doi.org/10.1016/j.engstruct.2017.02.044